Study of the momentum distribution of a Zn single crystal using neutron Compton scattering

2000 J. Phys.: Condens. Matter 12 4293

(http://iopscience.iop.org/0953-8984/12/18/314)

J. Phys.: Condens. Matter **12** (2000) 4293–4302. Printed in the UK PII: S0953-8984(00)11827-2

Study of the momentum distribution of a Zn single crystal using neutron Compton scattering

D Nemirovsky†, R Moreh†, K H Andersen‡ and J Mayers‡
† Physics Department, Ben-Gurion University of the Negev, Beer-Sheva, Israel
‡ Rutherford Appleton Laboratory, Chilton, Didcot, Oxon OX11 0QX, UK

Received 14 February 2000

Abstract. The neutron Compton scattering technique (NCS) was used for measuring the atomic momentum distribution, at ∼4.6 K, of an hcp zinc single crystal in directions parallel and perpendicular to the hexagonal planes. A strong anisotropy has been observed and interpreted in terms of the anisotropic binding of the atoms in Zn. The data were used for deducing the zero-point mean-square atomic momenta $\langle p_x^2 \rangle$ and $\langle p_z^2 \rangle$. These were combined with reported measured values of $\langle x^2 \rangle$ and $\langle z^2 \rangle$ obtained by the Mössbauer effect and used to test the predictions of the uncertainty principle for the two products $\langle p_x^2 \rangle \langle x^2 \rangle$ and $\langle p_z^2 \rangle \langle z^2 \rangle$ near 0 K. The measured values of $\langle p_x^2 \rangle$ and $\langle p_z^2 \rangle$ seem to conform to the requirements of the uncertainty relations to within 3%. The data are compared with those obtained using the nuclear resonance photon scattering (NRPS) technique.

1. Introduction

The NCS technique has been used [1–3] for studying anisotropic systems such as that of a highly oriented pyrolytic graphite (HOPG) sample, and the mean-square linear momenta $\langle p_a^2 \rangle$ and $\langle p_c^2 \rangle$ along and perpendicular to the hexagonal planes of the C atoms were measured. In graphite, the atoms are of small mass and the binding between the atoms is very strong, hence the atomic momenta are very high leading to effective temperatures: $T_a \sim 900$ K and $T_c \sim 500$ K at $T = 295$ K in directions parallel and perpendicular to the graphite planes. The excess kinetic energies of the C atoms above that of room temperature is contributed by the very high *zero-point* linear momenta of the atoms in HOPG.

In the present work, we used the NCS technique to study a single crystal sample of metallic zinc. In analogy with HOPG, metallic Zn is also anisotropic, having a hexagonal closed packed (hcp) structure with a high c/a-ratio of 1.861, whereby the atomic binding in the hexagonal planes is stronger than that along the c-axis. In the case of Zn, the atomic mass is ∼5.5 times higher than that of carbon and the expected intrinsic accuracy of the measured atomic momenta using the NCS process becomes much lower.

The purpose of the present work is threefold: first, to deduce the anisotropic binding properties of the Zn atoms in a metallic single crystal by measuring the zero-point mean-square linear momenta $\langle p_a^2 \rangle$ and $\langle p_c^2 \rangle$ of the Zn atoms along and normal to the hexagonal planes of the single crystal; second, to find out the sort of accuracy which can be achieved by applying the NCS technique to a sample having a mass 5.5 times higher than that of carbon; third, to combine the values of $\langle p_a^2 \rangle$ and $\langle p_c^2 \rangle$ of Zn with those of $\langle x^2 \rangle$ and $\langle z^2 \rangle$ (obtained using the Mössbauer effect) in order to test whether the products $\langle p_x^2 \rangle \langle x^2 \rangle$ and $\langle p_z^2 \rangle \langle z^2 \rangle$ conform to the requirements of the uncertainty principle near 0 K.

0953-8984/00/184293+10$30.00

To date, only two techniques have been employed for measuring the zero-point mean-square linear momenta of atoms: neutron Compton scattering (NCS) and nuclear resonance photon scattering [4] (NRPS). It is of interest to compare the results obtained by the two techniques. Note that while in the NRPS measurement, only the zero-point mean-square linear momentum, namely $\langle p_a^2 \rangle$ or $\langle p_c^2 \rangle$ is measured, the NCS technique yields a more detailed information, where the entire zero-point momentum *distribution* of the atoms along any direction in the sample is determined.

In a previous work [4], the NRPS technique has been employed to measure the anisotropy in the mean-square linear momenta of Zn atoms in a metallic single crystal, between 12 K and 530 K. From the results, the zero-point mean-square linear momenta $\langle p_a^2 \rangle$ and $\langle p_c^2 \rangle$ of ^{68}Zn were deduced. This was done by measuring the resonance scattering intensities from the 7362 keV level in ^{68}Zn with the photon beam parallel and normal to the hexagonal planes of the single crystal as explained in detail in [4].

2. The neutron Compton scattering technique

In this method, epithermal neutrons (in the eV range), scattered from a sample, act as monitors of the momentum distributions and of the kinetic energies (including the part due to the zero-point motion) of the scattering atoms. Experimentally, one measures the time of flight (TOF) of the epithermal neutrons from the pulsed source to the detector after scattering by the atoms of the sample. The TOF is measured alternately with and without a U absorber set in front of the n-detectors. The n-absorption dip corresponds to the first resonance energy at 6671 meV in ^{238}U which defines the final energy of the scattered neutron.

When the sample is highly anisotropic, such as an hcp Zn single crystal, the zero-point mean-square atomic momenta of the atoms are expected to have maximum and minimum values, $\langle p_a^2 \rangle$ and $\langle p_c^2 \rangle$. In most cases, the mean-square atomic momenta are expressed in terms of the effective temperatures T_a and T_c which are related to each other by:

$$\langle p_a^2 \rangle = MkT_a \text{ and } \langle p_c^2 \rangle = MkT_c \tag{1}$$

where M is the mass of the scattering atom and k the Boltzmann constant. These values correspond to the motion of the Zn atoms in directions parallel and perpendicular to the hexagonal planes of the crystal. The extent of the anisotropy in the motion of the Zn atoms may be illustrated by noting that a recent NRPS measurement on the ^{68}Zn isotope [4] yielded: $T_a = 100.5$ K and $T_c = 62.6$ K at $T = 12$ K. The increment of T_a and T_c over 12 K is due to a quantum effect and is contributed by the *zero-point* motion of the Zn atoms in the single crystal. It may be noted that a strong atomic binding along the hexagonal planes implies a large zero-point mean-square linear momentum $\langle p_a^2 \rangle$ and hence a small zero-point mean-square atomic displacement $\langle x_a^2 \rangle$, while a weak atomic binding along the c-axis implies a correspondingly small $\langle p_c^2 \rangle$ and hence a large $\langle x_c^2 \rangle$. In fact, the zero-point mean-square displacements were measured using the Mössbauer effect [5, 6] and were found to be in the ratio $\langle x_c^2 \rangle / \langle x_a^2 \rangle = 1.57$. At any intermediate direction making an angle θ with the c-axis, the effective temperature is related to T_c and T_a by:

$$T_\theta = T_a \sin^2 \theta + T_c \cos^2 \theta. \tag{2}$$

In poly-crystalline Zn, there is no preferred direction and the measured effective temperature T_e along any direction of the sample is related to the directional effective temperatures T_a and T_c by: $T_e = (2T_a + T_c)/3$. The value of T_e was measured experimentally [7] for the ^{68}Zn isotope in a natural Zn sample, kept at $T = 12$ K, using the NRPS method and found to be $T_e = 87.9$ K. When this value is corrected for the average mass of natural Zn, one obtains: $T_e = 89.7$ K.

In the NCS technique one measures a Compton profile curve whose standard deviation σ_a is related to the effective temperature T_a by $T_a = h^2\sigma_a^2/(4\pi^2 Mk)$. A similar equation holds for T_c. Here also, at any direction making an angle θ with the c-axis, the standard deviation σ_θ fulfils the relation:

$$\sigma_\theta^2 = \sigma_a^2 \sin^2\theta + \sigma_c^2 \cos^2\theta \tag{3}$$

transferring momentum $\boldsymbol{Q}$ and energy ε by scattering from an atom of mass M. If the momentum of the atom is $\boldsymbol{p}$ before collision, then momentum conservation requires that it is $\boldsymbol{p}+\boldsymbol{Q}$ after collision, and to conserve kinetic energy, the equation: $\varepsilon = [(\boldsymbol{p}+\boldsymbol{Q})^2 - \boldsymbol{p}^2]/2M$ must be satisfied. The component of atomic momentum along $\boldsymbol{Q}$ is given by: $y = (2m\varepsilon - \boldsymbol{Q}^2)/2Q$. Thus by measuring ε and Q along a certain direction, it is possible to deduce $J(Q, y)$, which is related to the probability that the atomic momentum component along Q is y. Experimentally, the distributions of the Zn atomic momenta, $J(Q_a, y)$ and $J(Q_c, y)$ in directions parallel and normal to the hexagonal planes were measured, from which the effective temperatures T_a and T_c were deduced. In our analysis we have accounted for the final state effects that were discussed in detail in [9].

3. Experimental method

The neutron Compton scattering measurements were performed using the ISIS pulsed neutron source of the Rutherford Appleton Laboratory in the UK in conjunction with the electron-volt spectrometer (EVS). The experimental system consisted of a scattering chamber, a cryostat, a single crystal of metallic Zn, and four banks of n-detectors (figure 1). Two metallic Zn single crystals were used in the course of the measurements, each with dimensions $40 \times 20 \times 2$ mm^3, the first cut with its 40×20 mm^2 plane normal to the crystal c-axis, and the second cut with its 40×20 mm^2 plane parallel to the hexagonal planes of the crystal. The Zn sample was held in the middle of a square aluminium frame using thin Al foils; it was placed with its plane at an angle of 45° with respect to the incident n-beam (figure 1). The geometry of the system was such that the neutron beam did not hit the Al frame to avoid increasing the background. Each of the four detector banks consisted of eight Li-glass scintillators. The banks were placed nearly symmetrically on both sides of the n-beam, one of which corresponds to a transmission geometry while the other one corresponds to a reflection geometry (labelled 'T' and 'R' in figure 1). The detector angles in one bank were between 78 and 102° (figure 1) while the other two were placed at backward angles, between 135 and 150°. Figure 1 depicts the linear momenta $\boldsymbol{k}_i$, $\boldsymbol{k}_r$ and $\boldsymbol{k}_t$ of the incident and the scattered neutrons, at ∼90 and at ∼270° corresponding to reflection and transmission geometries respectively. The momentum transferred by the scattering nuclei, $\boldsymbol{Q}_c$ and $\boldsymbol{Q}_a$ for the last two geometries are also indicated.

The time of flight (TOF) of neutrons is measured from the moderator to each of the 32 n-detectors after scattering from the Zn sample. The moderator–scatterer distance is ∼11.0 m while the scatterer–detector distance is ∼0.5 m. A difference resonance foil absorber technique is used for defining the final energy of the neutrons [10]. The absorbing foil used in the present measurement is uranium whose resonance energy is 6671 meV, having a Lorentzian shape, with a half width at half maximum (HWHM) of 63 meV. The use of a U foil absorber is more advantageous than that of gold, because of its higher resonance energy and narrower HWHM than that of gold (being 4912 meV and 138 meV). This means that U provides both higher momentum transfers and better energy resolution, enabling higher accuracy in measuring the effective temperatures. The main drawback in using a U foil is that the resulting counting rate is ∼10 times lower than that of a gold foil.

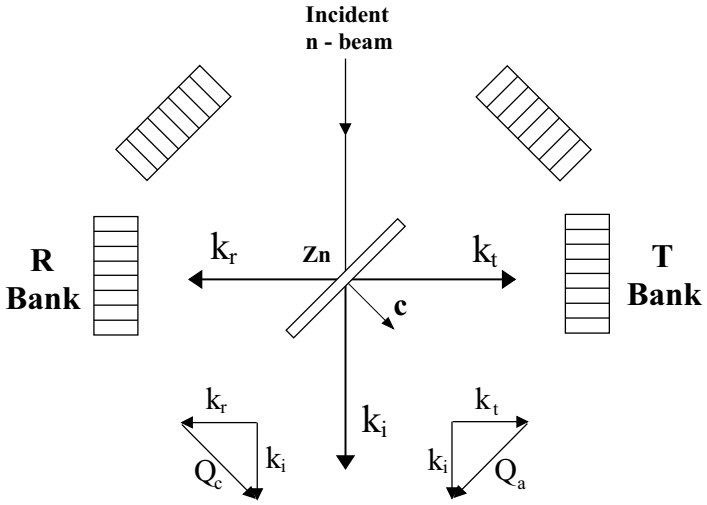

Figure 1. Schematic diagram of the experimental system showing the incident n-beam, the Zn sample and four banks each containing eight n-detectors). R and T denote detector banks set along the directions of the *reflected* (R) and *transmitted* (T) neutrons with respect to the hexagonal planes of the Zn single crystal. k_i is the linear momentum of the incident neutrons; k_t and k_r are those of the scattered neutrons corresponding to momentum transfers Q_a and Q_c along and perpendicular to the hexagonal planes of the Zn sample. The relations between the vectors of the scattering process for each of the two geometries are shown in the lower part of the figure.

The TOF spectra of neutrons scattered by the Zn single crystal, kept at 4.6 K, were taken with and without the U resonance absorber placed in front of the n-detectors. More details concerning the eVS spectrometer can be found elsewhere [11]. With the above geometric arrangement it was possible to simultaneously cover the momentum distribution of the Zn atoms in directions parallel and normal to the Zn hexagonal planes, and at several intermediate angles. A total beam charge of around 4000 μA h protons on the spallation target was accumulated per 24 h for each TOF spectrum measured. Calibration runs were taken by using a powdered Pb scatterer and measuring its well known n-diffraction lines at thermal neutron energies. Figure 2 shows typical TOF spectra of neutrons scattered from the Zn single crystal as measured by two detectors, at 92.5 and 269.5° corresponding to reflection and transmission geometries. These detectors depict the distribution of atomic momenta of the Zn atoms along and normal to the hexagonal planes showing a remarkable difference in the width obtained in the two cases. Note that the line width is largely contributed by the instrumental resolution, having a full width at half maximum of 3.99 μs, and is of practically the same size for the two detectors.

It is important to add that in fitting the Compton profile function $J(y)$, we accounted for the fact that the natural Zn sample contains five different isotopic masses, of natural abundance (^{64}Zn 48.6%, ^{66}Zn 27.9%, ^{67}Zn 4.1%, ^{68}Zn 18.8%, ^{70}Zn 0.6%) having different scattering cross sections. The fitted peak is thus a sum of five peaks each weighted by the product of its natural abundance and its scattering cross section. Since all the Zn isotopes have the same inter-atomic potential, the linear momenta are expected to vary with isotopic mass as $M^{1/4}$ and hence only one fitting parameter is needed for all isotopes. Thus the effective resolution function for Zn is slightly broadened compared to the case of a mono-isotopic sample. It may be noted that the average difference in TOF from two neighboring isotopes is only 0.2 μs out of a total of $\sim$300 μs. The instrumental resolution of the eVs spectrometer for a U resonance absorber varied between 10 Å^{-1} and 15 Å^{-1} depending on the scattering angle. However,

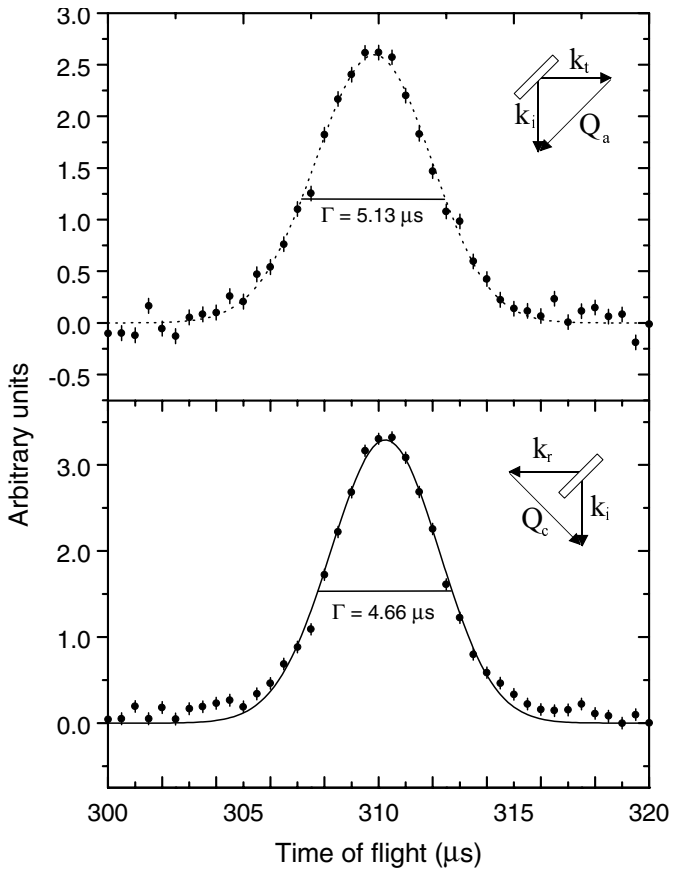

Figure 2. Typical measured TOF spectra (data bars) of neutrons scattered by the single crystal of Zn, with momentum transfers parallel (lower figure) and normal (upper figure) to the hexagonal planes as detected at ∼90 and ∼270°. Solid lines through the data points are best fits which accounted for the instrumental resolution function and the final state effects. The half widths at half maximum of the TOF spectra are indicated. Note that the instrumental resolution width is 3.99 μs and is the same for the two spectra.

the small mass correction was taken into account to obtain an accurate value of the zero-point linear momentum from $J(y)$. Multiple scattering of neutrons in the sample was calculated by accounting for the sample thickness and its geometry with respect to the n-beam and found to be negligible.

4. Results and discussion

In the following discussion, all quantities measured at ∼4.6 K, such as the linear momenta or displacements will be referred to as the zero-point quantities. This is justified by noting that zero-point effective temperatures T_a and T_c are much higher than 4.6 K, and the error introduced by this approximation is negligible.

Data analysis was performed by fitting the TOF spectra with the neutron Compton profile function $J(y)$ after convoluting with a Voigtian instrumental function and including final state effects. The incorporation of those effects into the calculation is discussed in more detail elsewhere [11].

It should be emphasized that the inclusion of the FSEs in the case of Zn has a very small effect on the calculated TOF spectra and a negligible effect on the resulting width of the momentum distribution. This point is illustrated in figure 3 where the calculated TOF spectra (the dotted and solid lines) are shown with and without the inclusion of FSEs. The two lines are almost indistinguishable and their difference is shown in figure 3 as a dashed line after being enlarged by a factor of five. This gives an idea about the magnitude of the FSEs in Zn in the case where a U resonance absorber is used.

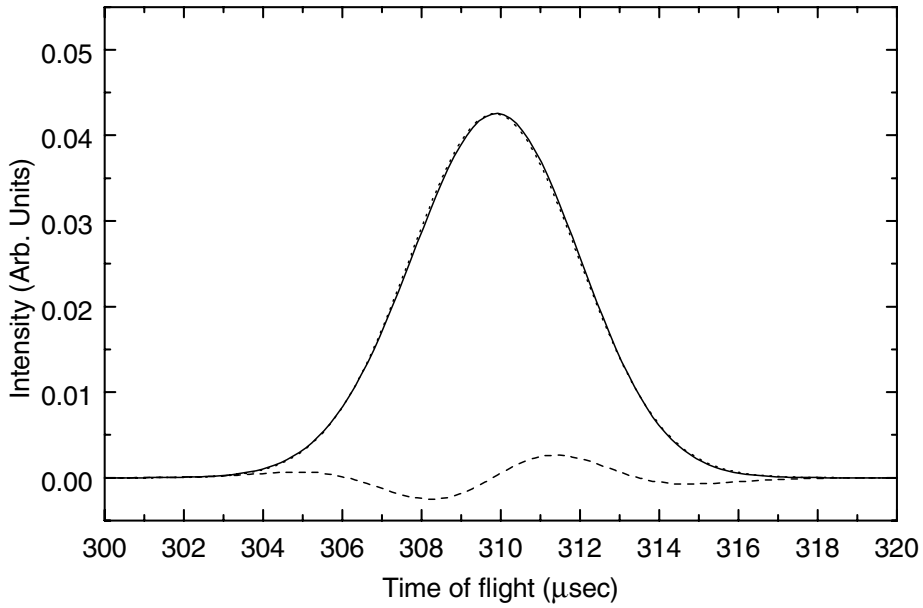

Figure 3. Calculated TOF spectra for a Zn sample (assuming $A = 65.39$) where final state effects (FSEs) were taken into account (dotted line). The solid line does not include the FSEs. The dashed line is the difference between these two calculated spectra (after being enlarged by a factor of five).

The values of σ_θ (in Å^{-1} units) of the Compton profile functions obtained from the fits to the TOF spectra of 31 detectors are shown in figure 4 versus the angle θ between the Zn single crystal c-axis and the momentum transfer vector $\boldsymbol{Q}$. These data were then best fitted using equation (3) and the values of σ_a and σ_c were obtained, from which T_a and T_c at 4.6 K for metallic Zn were deduced. The above measurements were repeated three times on entirely two different sets of runs. The results for one run are shown in figure 4. It reveals a strong anisotropy as seen from the clear separation between the values of σ along and normal to the hexagonal planes of the Zn single crystal. Note that all values are given for a Zn mass of 65.39 amu which is the average mass of natural Zn. The average results of T_a, T_c for the three runs together with the weighted average are given in table 1. For comparison, the values measured by the nuclear resonance photon scattering (NRPS) technique [4] on ^{68}Zn (corrected to $M = 65.39$ by applying an $M^{-1/2}$ mass correction) are also given. The table also lists the effective temperature T_e at $T = 0$ K, of a polycrystalline Zn sample, which was deduced from the measured T_a and T_c, using: $T_e = (2T_a + T_c)/3$. It is interesting to note that the present NCS values of T_a, T_c and T_e are higher by $\sim$3% but agree within error with the NRPS values (table 1). Moreover, both sets of values are higher but in reasonable agreement with $T_e = 87.0$ K, 87.8 K and 85.8 K, deduced from the theoretical and experimental phonon

spectra [12–14] $g(\nu)$ of metallic Zn, respectively, by using the relation:

$$T_e = \int_0^{\nu_m} g(\nu) h\nu\alpha \, \mathrm{d}\nu \Big/ \left(k \int_0^{\nu_m} g(\nu) \, \mathrm{d}\nu \right) \tag{4}$$

with $\alpha = [(\mathrm{e}^{h\nu/kT} - 1)^{-1} + 1/2]$, and ν_m the maximum cutoff frequency of the phonon spectrum.

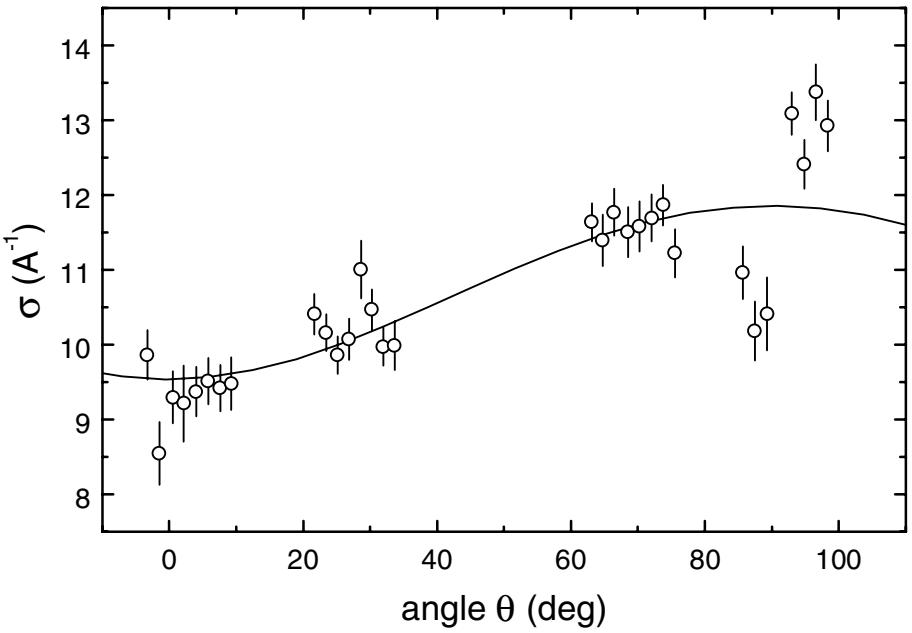

Figure 4. Measured standard deviations of the Compton profile curves versus the angle θ between the Q-vector and the normal to the hexagonal planes of Zn. The solid line is a fitted curve of the form: $\sigma_\theta^2 = \sigma_a^2 \sin^2\theta + \sigma_c^2 \cos^2\theta$. The values of T_c and T_a for Zn were deduced from σ_a^2 and σ_c^2 (see text).

Table 1. Measured effective temperatures T_a and T_c of a Zn single crystal, at 4.6 K using the NCS method, in directions parallel and perpendicular to the hexagonal planes. The results of three separate experiments are listed and are corrected for a Zn atomic mass, $M = 65.39$ amu, where the errors are enclosed in parentheses. The quoted results of the NRPS method [4] (originally measured in ^{68}Zn) were also corrected to an atomic mass of 65.39 amu.

	NCS I	NCS II	NCS III	$(\mathrm{NCS})_{av}$	NRPS	[12]	[13]	[14]
T_a (K)	100.1(2.5)	107.7(1.8)	105.3(2.8)	104.1(2.3)	102.5(5.0)			
T_c (K)	68.0(1.1)	69.7(1.4)	64.8(4.2)	68.1(1.7)	63.9(3.1)			
T_e (K)	89.4(2.0)	95.0(1.7)	91.8(3.3)	92.1(2.1)	89.6(4.4)	87.0	87.8	85.8

In the following we deal with the above results in view of the expectations of the uncertainty principle (UP). To do so, we express our measured effective temperature in terms of the mean-square linear momenta using the relations given in equation (1). Table 2 lists those results and shows that $\langle p_a^2 \rangle$ is ∼60% larger than $\langle p_c^2 \rangle$. These data may be contrasted with the mean-square linear displacements $\langle x_a^2 \rangle$ and $\langle x_c^2 \rangle$ along and normal to the hexagonal planes (measured using the Mössbauer effect) where $\langle x_a^2 \rangle$ was found to be *smaller* by ∼60% than $\langle x_c^2 \rangle$. This behaviour is expected in view of the UP which requires the products $\langle p_a^2 \rangle \langle x_a^2 \rangle$ and $\langle p_c^2 \rangle \langle x_c^2 \rangle$ at 0 K to

conform to the uncertainty relations, namely,

$$\langle p_a^2\rangle\langle x_a^2\rangle \geqslant h^2/16\pi^2 \tag{5}$$

$$\langle p_c^2\rangle\langle x_c^2\rangle \geqslant h^2/16\pi^2. \tag{6}$$

It should be pointed out that the Mössbauer measurements were carried out at ∼4.4 K, by two groups of investigators using the 93.3 keV level of the ^{67}Zn isotope. In table 2, the average of these values are listed after being normalized to an atomic mass $M = 65.39$.

Table 2. Mean-square atomic momenta $\langle p_a^2\rangle$ and $\langle p_c^2\rangle$ along the a-axis and the c-axis of a Zn single crystal as measured in the present NCS work and using the NRPS technique [4]. The measured and calculated values for a metallic polycrystalline Zn sample are also given. The average values of $\langle x_a^2\rangle$ and $\langle x_c^2\rangle$ were taken from Mössbauer measurements [5, 6]. The calculated values of $\langle x^2\rangle$ and $\langle p^2\rangle$ were deduced from the phonon spectra [12–14]. The products $\langle p^2\rangle\langle x^2\rangle$ for the various cases are given in units of $(9/8)h^2/16\pi^2$. The errors are enclosed in parentheses and the units of the various symbols are enclosed in square brackets.

	$\langle p^2\rangle$ [Å^{-2}] Present	$\langle p^2\rangle$ [Å^{-2}] NRPS	$\langle x^2\rangle$ [10^{-3}Å^2] Mossbauer	$\langle p^2\rangle\langle x^2\rangle$ [$(9/8)h^2/16\pi^2$] Present	$\langle p^2\rangle\langle x^2\rangle$ [$(9/8)h^2/16\pi^2$] NRPS
Measured					
a-axis	140.2(3.0)	138.0(6.7)	2.058(0.041)	1.025(0.030)	1.009(0.053)
c-axis	91.7(2.2)	86.1(4.1)	3.234(0.316)	1.053(0.106)	0.988(0.108)
Polycrystal	124.0(2.8)	120.7(5.8)	2.450(0.147)	1.034(0.055)	1.002(0.071)
Calculated (polycrystalline Zn)					
[12]	117.3		2.56	1.0637	
[13]	118.2		2.60	1.0899	
[14]	115.6		2.76	1.1338	

The most interesting point in equations (5) and (6) is to find out to what extent the product of the uncertainties for a real solid approaches the lowest limit of the uncertainty principle, namely, to find out when the equality sign is achieved. Theoretically, only a harmonic oscillator in its ground state fulfils the equality sign. Thus an Einstein solid, at 0 K, represented as a system of harmonic oscillators having a single frequency is expected to fulfil the equality sign. However, a real harmonic solid with a frequency distribution $g(\nu)$ at 0 K, yields a higher effective value for the product. This may be seen by first evaluating $\langle x_a^2\rangle$ and $\langle p_a^2\rangle$ using the ground state Gaussian wave function of a harmonic oscillator and integrating over $g(\nu)$ yielding:

$$\langle x_a^2\rangle = (h/8\pi^2 m)\int_0^{\nu_m} g(\nu)\nu^{-1}\,\mathrm{d}\nu \Big/ \left(\int_0^{\nu_m} g(\nu)\,\mathrm{d}\nu\right) = (h/8\pi^2 m)M_{-1} \tag{7}$$

$$\langle p_a^2\rangle = (hm/2)\int_0^{\nu_m} g(\nu)\nu\mathrm{d}\nu \Big/ \left(\int_0^{\nu_m} g(\nu)\,\mathrm{d}\nu\right) = (hm/2)M_{+1}. \tag{8}$$

This yields for the product, the following expression:

$$\langle x_a^2\rangle\langle p_a^2\rangle = (h^2/16\pi^2)M_{-1}M_{+1} \tag{9}$$

where M_{-1} and M_{+1} are the $n = -1$ and $n = +1$ moments of the phonon spectrum of the solid. A similar expression may be written for $\langle x_c^2\rangle$ and $\langle p_c^2\rangle$. The above product may be calculated for an anisotropic Debye solid which may be represented by two different phonon spectra $g_a(\nu)$ and $g_c(\nu)$ (each obeying the relation $g(\nu) \propto \nu^2$), yielding:

$$\langle p_a^2\rangle\langle x_a^2\rangle \geqslant (9/8)h^2/16\pi^2 \tag{10}$$

$$\langle p_c^2\rangle\langle x_c^2\rangle \geqslant (9/8)h^2/16\pi^2. \tag{11}$$

It is of interest to test to what extent our measured values of $\langle p_a^2 \rangle$ and $\langle p_c^2 \rangle$ fulfil the later relation if $\langle x_a^2 \rangle$ and $\langle x_c^2 \rangle$ are taken from the Mössbauer data. The results are listed in the last two columns of table II and are given in units of $(9/8)h^2/16\pi^2$. It may be seen that any product which is larger than 1.0 in such units indicates a deviation from the lowest limit of the uncertainty principle for a Debye solid. Thus the present NCS results are on average higher by around 3% but conform within error with the requirements of the UP. A somewhat closer agreement with the predictions of the UP was obtained in our previous work using the NRPS method [4].

In the literature no information about the phonon spectra of a Zn *single crystal* was reported and the only information was for a polycrystalline metallic Zn. Thus in order to make another comparison of the NCS results with the predictions of the uncertainty principle, we deduced the value of $\langle p^2 \rangle$ and $\langle x^2 \rangle$ for a polycrystalline Zn using the following relations:

$$\langle p^2 \rangle = (2\langle p_a^2 \rangle + \langle p_c^2 \rangle)/3 \tag{12}$$

$$\langle x^2 \rangle = (2\langle x_a^2 \rangle + \langle x_c^2 \rangle)/3. \tag{13}$$

The deduced product $\langle p^2 \rangle \langle x^2 \rangle$ which is based on the present NCS data is higher by ∼3% than that predicted for a Debye solid (see table 2). This value should also be compared with those calculated using the $n = -1$ and $n = +1$ moments (equations (7) and (8)) of the real phonon spectra [12–14] for a polycrystalline Zn sample (table 2). It may be seen that the NCS-based value is *lower* by ∼4% than that based on the theoretical phonon spectra [12, 13]. This deviation increases to 10% when the NCS result is compared with that based on the experimental phonon spectrum [14].

A few conclusions emerge from a consideration of table 2. First, the present measured values of $\langle p_a^2 \rangle$ and $\langle p_c^2 \rangle$ are higher by ∼2.7%, but practically the same as those obtained using the NRPS method. A similar agreement to within ∼3% occurs between the present NCS results and those predicted for a Debye solid. This shows that an anisotropic Debye solid is a good representation of a Zn single crystal. Second, the measured NCS value of $\langle p^2 \rangle$ is higher by ∼5% than the average deduced from the theoretical phonon spectra [12, 13] using equation (7). This deviation increases further when the comparison is made with the experimental phonon spectrum. Third, an opposite situation occurs for the case of $\langle x^2 \rangle$. Here the Mössbauer value of $\langle x^2 \rangle$ is *lower* by ∼5% than that deduced from the theoretical phonon spectrum. The deviation increases to 13% when the comparison is made with the $\langle x^2 \rangle$ based on the experimental phonon spectrum [14]. Here, the large deviation may be caused by the high sensitivity of $\langle x^2 \rangle$ to small variations in $g(\nu)$ at the lowest vibrational frequencies (see equation (8)). Such errors have practically no effect on $\langle p^2 \rangle$ which is governed mainly by the higher vibrational frequencies. Thus the high value of the product $\langle p^2 \rangle \langle x^2 \rangle$ deduced from the phonon spectra could be due to the large predicted value of $\langle x^2 \rangle$ caused by some error in the low frequency limit of $g(\nu)$.

Another explanation for the above may be invoked by considering the dimensionality of the sample which is expected to play an important role in the determination of the lowest achievable value of the product $\langle p^2 \rangle \langle x^2 \rangle$. To do so we may consider the case of highly oriented pyrolytic graphite known to be a highly anisotropic layered system and a good example of a two-dimensional system. When the product $\langle p^2 \rangle \langle x^2 \rangle$ is calculated at 0 K for graphite using its phonon spectrum [15, 16] we obtain $\langle p^2 \rangle \langle x^2 \rangle \sim 1.43$ in units of $(9/8)h^2/16\pi^2$. Similar values were obtained when the product was calculated for the a-direction and the c-direction of HOPG using the calculated phonon spectra of [17]. Such values represent a huge deviation from that of a Debye solid.

5. Conclusions

We have shown that the NCS technique may be used for measuring the zero-point momentum distributions for masses as heavy as zinc with an error of the order of 5%. This was possible because use was made of a U foil absorber to define the final energy of the neutron. The width of the neutron resonance capturing level in U is much narrower than that of a gold foil. The deduced zero-point effective temperatures are of about the same accuracy as those obtained using the nuclear resonance photon scattering technique. The measured zero-point mean-square linear momenta $\langle p_a^2 \rangle$ and $\langle p_c^2 \rangle$ along and perpendicular to the Zn hexagonal planes were combined with the literature values of the zero-point mean-square displacements obtained using the Mössbauer effect. The products of the form $\langle p_a^2 \rangle \langle x_a^2 \rangle$ and $\langle p_c^2 \rangle \langle x_c^2 \rangle$ were found to conform to the requirements of the uncertainty principle for a Debye solid to within $\sim$3%.

References

[1] Fielding A, Timms D N and Mayers J 1998 *Europhys. Lett.* **44** 255
[2] Mayers J, Burke T M and Newport R J 1994 *J. Phys.: Condens. Matter* **6** 641
[3] Rauh H and Watanabe N 1984 *Phys. Rev. Lett.* A **100** 244
[4] Moreh R and Fogel M 1994 *Phys. Rev.* B **50** 16 184
[5] Potzel W, Adlassnig W, Narger U, Obenhuber T, Riski K and Kalvius G M 1984 *Phys. Rev.* B **30** 4980
Potzel W 1993 *Mössbauer Spectroscopy Applied to Magnetism and Materials Science* vol 1, ed G J Long and F Grandjean (New York: Plenum) p 305
[6] Pound R V, Niesen L, De Waard H and Zhang Gui-Lin 1984 *Phys. Rev.* **55** 190
[7] Moreh R and Shahal O 1989 *Nucl. Phys.* A **491** 45
[8] Mayers J 1991 *Phys. Rev.* B **41** 41
[9] Sears V F 1984 *Phys. Rev.* B **30** 44
[10] Newton R 1981 *Scattering Theory of Waves and Particles* (Berlin: Springer)
[11] Brugger R M, Taylor A D, Olson C E, Goldstone J A and Soper A K 1984 *Nucl. Instrum. Methods* **221** 393
[12] Raubenheimer L J and Gilat G 1967 *Phys. Rev.* **157** 586
[13] Chesser N J and Axe J D 1974 *Phys. Rev.* B **9** 4060
[14] Eremeev I P, Sadikov I P and Chernyshov A A 1976 *Sov. Phys.–Solid State* **18** 960
[15] Nicklow R, Wakabayashi N and Smith H G 1972 *Phys. Rev.* B **5** 4951
[16] Al-Jishi R and Dresselhaus G 1982 *Phys. Rev.* B **26** 4515
[17] Young J and Koppel J U 1965 *J. Chem. Phys.* **42** 357